IEEE Access
Multidisciplinary | Rapid Review | Open Access Journal

Received December 8, 2018, accepted January 9, 2019, date of publication February 19, 2019, date of current version March 12, 2019.

Digital Object Identifier 10.1109/ACCESS.2019.2897222

Robust GPS/INS/DVL Navigation and Positioning Method Using Adaptive Federated Strong Tracking Filter Based on Weighted Least Square Principle

HAILIANG XIONG, (Member, IEEE), ZHENZHEN MAI, (Student Member, IEEE), JUAN TANG, AND FEN HE

School of Information Science and Engineering, Shandong University, Qingdao Campus, Qingdao 266237, China

Corresponding author: Fen He (hefen@sdu.edu.cn)

This work was supported in part by the National Natural Science Foundation of China under Grant 61401253, in part by the Key Research and Development Program of Shandong Province under Grant 2017GGX201003, and in part by the National Key R&D Program of China under Grant 2018YFC0831006-2.

ABSTRACT Multi-sensor integrated positioning technique that combines complementary features of the global positioning system (GPS) and inertial navigation system (INS) for navigation in challenging urban environments has been a hot research area. A variety of algorithms have been proposed over the past two decades for this well-studied field. However, with the increasing demands of seamless positioning, traditional GPS/INS integrated technique faces rigorous challenges, especially in GPS-denied environment, where traditional techniques cannot be applied directly. To improve the precision and robustness of the navigation system, a novel hybrid GPS/INS/Doppler velocity log (DVL) positioning method is proposed, which introduces DVL as the reference information to assist the GPS module to correct the divergence error of INS. A new robust adaptive federated strong tracking Kalman filter (RAFSTKF) algorithm is also presented for data fusion, which has the advantage of robustness with respect to the uncertainty of the system model. Meanwhile, we introduce the least square principle and adaptively adjust information sharing factors to obtain the optimal estimation, which can improve the reliability of the overall system. The theoretical analysis and simulation results demonstrate the effectiveness of the proposed hybrid GPS/INS/DVL positioning method based on RAFSTKF. In addition, the tracking performance of the proposed method outperforms that of traditional federated Kalman filter.

INDEX TERMS Localization, target tracking, positioning, hybrid navigation, Kalman filter, weighted least square, federated strong tracking filter.

I. INTRODUCION

Many existing and perspective technologies of navigation and location systems would benefit notably from the ability to position accurately and reliably in challenging environments [1]–[6]. Recently, inertial navigation systems (INS) provide users with position, velocity, and attitude (PVA) information with high resolution independent of the vehicle platform [7], [8]. However the PVA information provided by INS can only maintain reliable precision for short time limited by the fact that the INS navigation error will accumulate over time and diverge after a long duration [9]. Global positioning system (GPS) is a satellite-based navigation system that provides a user with proper equipment access to useful and accurate real-time three-dimensional (3D) position and velocity information anywhere on the globe [10]. However, it is not only susceptible to multipath effect but also unable to effectively fulfill precise error correction in a wide range of driving areas [11]–[13]. Doppler velocity log (DVL) utilizing the doppler effect is an ideal sensor to get measurement speed in high precision and is easy to use [14]–[16]. Ultra-wideband (UWB) technology [17], [18] can provide a ranging accuracy of tens of centimeters with fine time resolution and has robustness against multipath interference,

The associate editor coordinating the review of this manuscript and approving it for publication was Shuai Han.

which makes UWB particularly attractive for dense multipath environments [19]–[21].

As these navigation sensors and technologies have complementary characteristics, integrated navigation system has become a hot research area and many researchers have proposed different combination methods to improve the navigation precision. In the past few decades, benefitting from overcoming each other's limitations and performance improvement, integrated GPS/INS system offering decimeter-to-centimeter-level relative positioning accuracy has become a standard approach in modern navigation area [22], [23]. It has been applied in many fields such as military and civilian aircrafts, land vehicles, ships and submarines, missiles and rockets, etc., whose advantages include decreasing the inertial errors in position and velocity, the calibration of gyros and accelerometers et al [24], [25]. To offer improved performance, researchers have studied the fusion of additional sensors for relative navigation. For example, Rad et al. improved the attitude and position obtained via INS by integration of its information, star tracker attitude measurements, and horizon sensor transformation matrix [26]. Wang *et al.* [27] presented a method for fusing data from INS, GPS and VisNav based on information filter to estimate the relative navigation information. Wang *et al.* [15] proposed a multi-sensor integrated navigation scheme based on INS, Celestial Navigation System (CNS) and DVL to improve the performance of autonomous navigation for Unmanned Surface Vehicles (USVs) [15].

Efficient implementation of estimating algorithm plays a crucial role in integrated navigation, also leads to cost reduction [28], [29]. In general, there are a number of different solutions to state estimation for navigation and positioning, making it often unclear to decide the optimal solutions [30]. Kalman filter (KF) is the most commonly used estimation technique for integrating signals from short-term high performance systems, like INS, with reference systems exhibiting long-term stability, like GPS. The well-known conventional KF providing optimal solution in the sense of minimum variance criterion requires an accurate system model and exact stochastic information [31]. However, in most situations, the system model has an unknown bias, which may degrade the performance of the KF and even may cause the filter to diverge [32]–[34]. Strong tracking filter (STF) proposed by Zhou *et al.* introduces a fading factor to constrain the innovation outputs of the filter to satisfy the orthogonality principle. It is an ideal substitution to KF owing to its strong robustness and tracking ability of mutation status [35]–[37]. Moderate computation complexity is another merit of STF. The federated filter (FF) is a near-optimal estimator for decentralized, multi-sensor data fusion. Its partitioned estimation architecture is based on theoretically sound information-sharing principles. FF consists of one or more sensor-dedicated local filters, generally operating in parallel, plus a master combining filter. The master filter periodically fuses the outputs of the local filters to get the global estimation.

In this paper, we propose a novel GPS/INS/DVL hybrid positioning method using robust adaptive federated strong tracking Kalman filter (RAFSTKF). One of the key contributions of our research is that we use 3D position information of GPS and 3D velocity information of DVL as the reference information to correct the INS navigation error at the same time. In addition, we also propose a RAFSTKF algorithm based on least square principle, which is capable of providing stable navigation information even when it is under poor conditions. The algorithm is comprised of the following parts: 1) local filter: we establish two local filters based on STF. The measurement input of the first local filter is the position information difference between INS and GPS, while the measurement input of the second local filter is the velocity information difference between INS and DVL. 2) master filter: master filter is based on adaptive weighted least square principle. We adaptively adjust the outputs of the two local filters by using information sharing factors to get the optimum estimation. 3) feedback: once the optimum estimation is obtained, we feed it back to the INS. Therefore the INS module outputs accurate navigation information. The proposed algorithm and architecture are assessed by simulations conducted through a self-developed platform which is capable of providing whole-procedure simulation from trajectory generation to performance evaluation. Simulation results demonstrate that the proposed federated GPS/INS/DVL system based on the RAFSTKF algorithm can improve the navigation accuracy significantly. In addition, we find that the sampling interval is an important factor related to the accuracy, in general the shorter the sampling interval is, the better the navigation result.

The remainder of the paper is organized as follows. In section II, we present brief introductions about the federated filter and strong tracking filter. Section III introduces the multi-sensor integrated navigation method using adaptive robust federated strong tracking Kalman filter algorithm. Simulation results are presented and the system performance is discussed in section IV, followed by the conclusions summarized in section V.

II. BASIC PRINCIPLE

A. FEDERATED FILTER

As depicted in Fig. 1, FF is a two-stage data processing technique in which the outputs of local sensor-related filters are subsequently processed and combined by a larger master filter [38]. We consider the system state vector X that propagates from (k-1)-th to k-th time instant according to the following dynamic model

$$X_k = F_{k,k-1}X_{k-1} + W_{k-1}. \tag{1}$$

The observation equation of i-th subsystem is given by

$$Z_{ik} = H_{ik}X_k + V_{ik}, \tag{2}$$

where $F_{k,k-1}$ is the system transition matrix and H_{ik} is the observation matrix. It should be noted that W_k and V_{ik} are process noise and measurement noise, respectively. W_k and V_{ik}

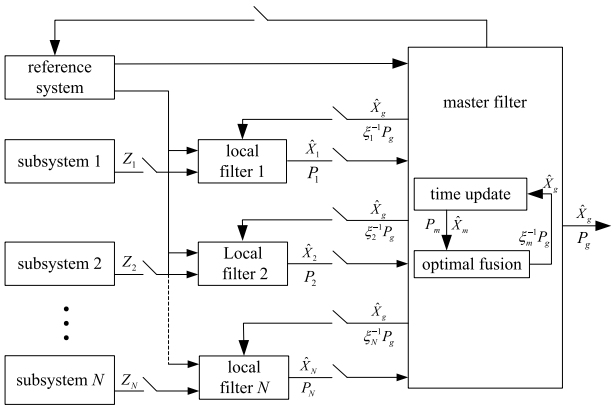

FIGURE 1. The general structure of federated filter.

satisfy the following statistical properties

$$E[W_k] = 0, \tag{3}$$
$$E[V_{ik}] = 0, \tag{4}$$
$$E\left[W_k V_{ik}^T\right] = 0, \tag{5}$$
$$E\left[W_k W_j^T\right] = Q_k \delta_{kj}, \tag{6}$$
$$E\left[V_{ik} V_{ij}^T\right] = R_{ik} \delta_{kj}, \tag{7}$$

where Q_k is the covariance matrix of process noise, R_{ik} is the covariance matrix of measurement noise, and δ_{kj} is the Kronecker-delta function.

Assuming the estimation outputs of N local filters are $\hat{X}_1, \hat{X}_2, \cdots, \hat{X}_N$ and the corresponding covariance matrices of estimation error are $P_1, P_2, \cdots, P_N$, then the information fusion of the master filter can be described as follows

$$P_g^{-1} = \sum_{i=1}^{N} P_i^{-1}, \tag{8}$$
$$\hat{X}_g = P_g \sum_{i=1}^{N} P_i^{-1} \hat{X}_i. \tag{9}$$

The feedback information from master filter to local filter is state estimation of master filter $\hat{X}_g$ and estimation covariance $\xi_i^{-1} P_g$. ξ_i is the information sharing factor which satisfies the following condition

$$\sum_{i=1}^{N} \xi_i = 1. \tag{10}$$

B. STRONG TRACKING FILTER

To improve the stability and enhance robustness for model uncertainty of traditional KF, we consider the STF algorithm. STF utilizes a suboptimal fading factor λ_k to decrease the influence of preceeding data, making the orthogonality principle (OP) valid all the way [39]

$$E\left[\gamma_{k+j} \gamma_k^T\right] = 0, \ k = 0, 1, 2, \cdots, \quad j = 1,2, \cdots, \tag{11}$$

where

$$\gamma_k = Z_k - H_k \hat{X}_{k,k-1}. \tag{12}$$

Hence, the STF methods can still provide reliable real-time tracking ability, estimate the position with satisfactory precision even when statistical information is not sufficient, and subsequently yield a predicted trajectory that matches the actual trajectory.

The covariance matrix of one step prediction of state error is modified as

$$P_{k,k-1} = \lambda_k F_{k,k-1} P_{k-1} F_{k,k-1}^T + Q_{k-1}. \tag{13}$$

Meanwhile, the gain matrix is transformed into the following form

$$K_k = P_{k,k-1} H_k^T \left[H_k P_{k,k-1} H_k^T + R_k\right]^{-1}. \tag{14}$$

As $P_{k,k-1}$ is related to λ_k, then K_k is also related to λ_k. According to [31], in order to deduce λ_k, we substitute (13) and (14) into (11)

$$P_{k,k-1} H_k^T \left[I - \left(H_k P_{k,k-1} H_k^T + R_k\right)^{-1} V_{ok}\right] = 0, \tag{15}$$

where

$$V_{ok} = E\left[\gamma_k \gamma_k^T\right]. \tag{16}$$

Then we get

$$\lambda_k H_k F_{k,k-1} P_{k-1} F_{k,k-1}^T H_k^T = V_{ok} - H_k Q_{k-1} H_k^T - R_k. \tag{17}$$

Here we define

$$M_k = H_k F_{k,k-1} P_{k-1} F_{k,k-1}^T H_k^T, \tag{18}$$
$$N_k = V_{ok} - H_k Q_{k-1} H_k^T - R_k. \tag{19}$$

The fading factor is determined by the following way [40]

$$\lambda_k = \begin{cases} \lambda_{0,k}, & \lambda_{0,k} \geqslant 1 \\ 1, & \lambda_{0,k} < 1 \end{cases} \tag{20}$$
$$\lambda_{0,k} = \frac{Tr(N_k)}{Tr(M_k)}. \tag{21}$$

Accordingly, V_{ok} can be given by

$$V_{ok} = \begin{cases} \gamma_1 \gamma_1^T, & k = 0 \\ \dfrac{\rho V_{ok-1} + \gamma_k \gamma_k^T}{1 + \rho}, & k \geqslant 1 \end{cases} \tag{22}$$

where ρ is a forgetting factor and $0.95 \leqslant \rho \leqslant 0.995$. Usually, we set ρ to be 0.95 as a rule of thumb [41].

The fading factor λ_k is of great importance in the STF method. Introducing λ_k helps to strength the effect of new information and decrease the influence of preceeding data, and keeps the convergence of the filter. Meanwhile, an appropriate value will increase the accuracy of the system and measurement models by minimizing the impact of obsolete data. When the mobile terminal (MT) moves with a high speed, we usually set $\lambda_k > 1$ to strengthen the effect of new information. When MT moves at a normal speed, we let $\lambda_k = 1$ owing to accuracy of the system and observation models, and STF becomes the standard KF at the moment [42].

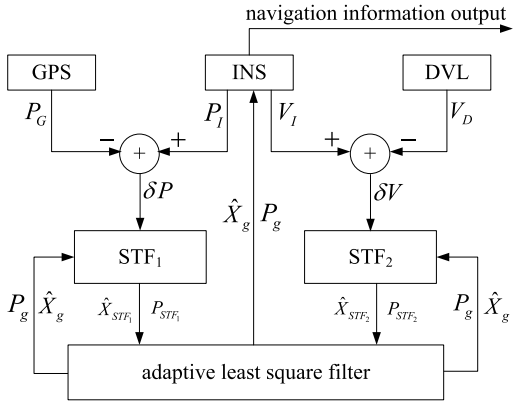

FIGURE 2. Diagram of GPS/INS/DVL navigation mechanism.

III. MULTI-SENSOR INTEGRATED NAVIGATION METHOD USING ADAPTIVE ROBUST FEDERATED STRONG TRACKING KALMAN FILTER ALGORITHM

Based on the introduction of navigation sensors in section I and the basic principle in section II, the multi-sensor integrated navigation method for GPS/INS/DVL using the adaptive robust federated strong tracking Kalman filter algorithm is proposed in this section. In this method, INS module acts as the main system, and GPS as well as DVL are introduced as subsystems. As a result, the GPS position information and the DVL velocity information are used to compensate INS navigation errors. The diagram of the multi-sensor integrated navigation method is shown in Fig. 2.

In consideration of gyro drifts and accelerometer biases, state variables of system can be defined as

$$X = [\phi_E \quad \phi_N \quad \phi_U \quad \delta V_E \quad \delta V_N \quad \delta V_U \quad \delta L \quad \delta\lambda \quad \delta h \quad \varepsilon_{rx} \quad \varepsilon_{ry} \quad \varepsilon_{rz} \quad \nabla_E \quad \nabla_N \quad \nabla_U]^T, \tag{23}$$

where ϕ_E, ϕ_N, ϕ_U are the attitude errors about east, north and vertical (up) axes of the platform, respectively. δV_E, δV_N, δV_U are the velocity errors along east, north and vertical direction, respectively. δL, $\delta\lambda$, δh are errors of latitude, longitude and height, respectively. ε_{rx}, ε_{ry}, ε_{rz} describe gyro drifts, and ∇_E, ∇_N, ∇_U represent accelerometer biases.

The system equation of local filter is

$$\dot{X}(t) = F(t)X(t) + W(t), \tag{24}$$

where $F(t)$ denotes state transition matrix, $W(t)$ is the system noise vector with the covariance matrix $Q(t)$.

The measurement equation of STF_1 is

$$Z_{1,k} = H_1 X_k + V_{1,k}, \tag{25}$$

where H_1 is the measurement matrix, $V_{1,k}$ is the measurement noise vector of STF_1 with the covariance matrix $R_{1,k}$.

$$H_1 = \begin{bmatrix} O_{3\times6} & I_{3\times3} & O_{3\times6} \end{bmatrix}. \tag{26}$$

$Z_{1,k}$, the difference between the position of INS and the position of GPS, is the observation of the measurement equation in STF_1, and it can be written as

$$Z_{1,k} = \begin{bmatrix} L_{INS} - L_{GPS} \\ \lambda_{INS} - \lambda_{GPS} \\ h_{INS} - h_{GPS} \end{bmatrix}. \tag{27}$$

The measurement equation of STF_2 is

$$Z_{2,k} = H_2 X_k + V_{2,k}, \tag{28}$$

where H_2 is the measurement matrix, $V_{2,k}$ is the measurement noise vector of STF_2 with the covariance matrix $R_{2,k}$.

$$H_2 = \begin{bmatrix} O_{3\times3} & I_{3\times3} & O_{3\times9} \end{bmatrix}. \tag{29}$$

$Z_{2,k}$, the difference between the velocity of INS and the velocity of DVL, is the observation of the measurement equation in STF_2, and it can be written as

$$Z_{2,k} = \begin{bmatrix} v_E^{INS} - v_E^{DVL} \\ v_N^{INS} - v_N^{DVL} \\ v_U^{INS} - v_U^{DVL} \end{bmatrix}. \tag{30}$$

Based on the system equation and measurement equation of STF_1, we get the optimum state estimation $\hat{X}_{1,k}$ of X and the covariance matrix of optimum state estimation error $P_{1,k}$ according to STF algorithm as summarized in Algorithm 1. Similarly $\hat{X}_{2,k}$ and $P_{2,k}$ can also be obtained from the algorithm based on system equation and measurement equation of STF_2. Then the estimated INS error results $\hat{X}_{i,k}(i = 1, 2)$ and the covariance matrix of optimum state estimation error $P_{i,k}(i = 1, 2)$ of the two local strong tracking filters are the input information of the main filter. In addition, we also put one step prediction of state $\hat{X}_{k,k-1}$ and covariance matrix of

Algorithm 1 the calculation process of STF

INITIALIZE (i represents i-th STF):
initial state vector $\hat{X}_{i,0}$ and covariance matrix $P_{i,0}$
CALCULATE(as for k moment):
Input: $\hat{X}_{k-1}$, $Z_{i,k}$, P_{k-1}, $F_{k,k-1}$, H_i, Q_{k-1}, $R_{i,k}$, $V_{i,0k-1}$, ρ_i;
Output:
1. one step prediction of state: $\hat{X}_{k,k-1} = F_{k,k-1}\hat{X}_{k-1}$;
2. residual of observation: $\gamma_{i,k} = Z_{i,k} - H_i\hat{X}_{k,k-1}$;
3. covariance of $\gamma_{i,k}$: $V_{i,0} = \frac{\rho V_{i,0k-1} + \gamma_{i,k}\gamma_{i,k}^T}{1+\rho_i}$;
4. calculation of $M_{i,k}$: $M_{i,k} = H_i F_{k,k-1} P_{k-1} F_{k,k-1}^T H_i^T$;
5. calculation of $N_{i,k}$: $N_{i,k} = V_{i,0k} - H_i Q_{k-1} H_i^T - R_{i,k}$;
6. calculation of $\lambda_{i,0k}$: $\lambda_{i,0k} = \frac{Tr(N_{i,k})}{Tr(M_{i,k})}$;
7. covariance matrix of one step prediction of state error: $P_{k,k-1} = \lambda_{i,k} F_{k,k-1} P_{k-1} F_{k,k-1}^T + Q_{k-1}$;
8. gain matrix: $K_{i,k} = P_{k,k-1} H_i^T \left[H_i P_{k,k-1} H_i^T + R_{i,k}\right]^{-1}$;
9. state estimation: $\hat{X}_{i,k} = \hat{X}_{k,k-1} + K_{i,k}\left[Z_{i,k} - H_i\hat{X}_{k,k-1}\right]$;
10. covariance matrix of state estimation error: $P_{i,k} = \left[I - K_{i,k}H_i\right] P_{k,k-1} \left[I - K_{i,k}H_i\right]^T + K_{i,k} R_{i,k} K_{i,k}^T$.

one step prediction of state error $P_{k,k-1}$ into the main filter to collaborate with $\hat{X}_{i,k}(i=1,2)$ and $P_{i,k}(i=1,2)$ to obtain the final optimum state estimation. The final estimation results are fed back and compensated to correct the INS navigation information. In the meantime, the final estimation results of the main filter are fed back to the two local filters.

In order to get the optimum fusion result, we first consider the direct fusion method. The error equation for one-step state prediction vector $\hat{X}_{k,k-1}$ can be given by

$$V_{\hat{X}_{k,k-1}} = \hat{X}_k^0 - \hat{X}_{k,k-1}. \tag{31}$$

The error equation for the outputs of STF_1 $\hat{X}_{1,k}$ becomes

$$V_{\hat{X}_{1,k}} = \hat{X}_k^0 - \hat{X}_{1,k}. \tag{32}$$

The error equation for the outputs of STF_2 $\hat{X}_{2,k}$ becomes

$$V_{\hat{X}_{2,k}} = \hat{X}_k^0 - \hat{X}_{2,k}, \tag{33}$$

where $\hat{X}_k^0$ is direct fusion value at the k-th moment.

Then the objective function on the basis of the least square principle can be written as follows

$$\min_{\{\hat{X}_k^0\}} \Omega_k = \min_{\{\hat{X}_k^0\}} V^T_{\hat{X}_{k,k-1}} P^{-1}_{k,k-1} V_{\hat{X}_{k,k-1}} + V^T_{\hat{X}_{1,k}} P^{-1}_{1,k} V_{\hat{X}_{1,k}} + V^T_{\hat{X}_{2,k}} P^{-1}_{2,k} V_{\hat{X}_{2,k}}. \tag{34}$$

Through the derivation of (34), we can get the constrained relationship of $\hat{X}_k^0$ as follows

$$\frac{d\Omega_k}{d\hat{X}_k^0} = 2V^T_{\hat{X}_{k,k-1}} P^{-1}_{k,k-1} + 2V^T_{\hat{X}_{1,k}} P^{-1}_{1,k} + 2V^T_{\hat{X}_{2,k}} P^{-1}_{2,k} = 0. \tag{35}$$

Transposing and simplifying above equation result in

$$P^{-1}_{k,k-1}(\hat{X}_k^0 - \hat{X}_{k,k-1}) + P^{-1}_{1,k}(\hat{X}_k^0 - \hat{X}_{1,k}) + P^{-1}_{2,k}(\hat{X}_k^0 - \hat{X}_{2,k}) = 0, \tag{36}$$

$$\hat{X}_k^0 = P_{\hat{X}_k^0}(P^{-1}_{k,k-1}\hat{X}_{k,k-1} + P^{-1}_{1,k}\hat{X}_{1,k} + P^{-1}_{2,k}\hat{X}_{2,k}), \tag{37}$$

and

$$P^{-1}_{\hat{X}_k^0} = P^{-1}_{k,k-1} + P^{-1}_{1,k} + P^{-1}_{2,k}, \tag{38}$$

where $P_{\hat{X}_k^0}$ is the covariance matrix of direct fused estimation error. As is shown in (37), $\hat{X}_k^0$ can be obtained in the fusion process of the main filter, and it's the global estimation of the state. Then the main filter distributes the global estimation information to each sub-filter according to the principle of information conservation as shown in Fig. 1. In the direct fusion filter, the sharing factor is a fixed value, which is the reciprocal of the sum of the local filters, and the change of state in dynamic environment is neglected.

In order to optimally balance the weights of the local filter information outputs and priori estimation based on the above system model, we can adaptively determine the weights according to the direct fusion results. As a result, we can get the final optimum state estimation. We establish the target function based on the least square principle

$$\min_{\{\hat{X}_k\}} \mathbb{T}_k = \min_{\{\hat{X}_k\}} \beta_{0,k}\left(\hat{X}_k - \hat{X}_{k,k-1}\right)^T P^{-1}_{k,k-1}\left(\hat{X}_k - \hat{X}_{k,k-1}\right) + \beta_{1,k}\left(\hat{X}_k - \hat{X}_{1,k}\right)^T P^{-1}_{1,k}\left(\hat{X}_k - \hat{X}_{1,k}\right) + \beta_{2,k}\left(\hat{X}_k - \hat{X}_{2,k}\right)^T P^{-1}_{2,k}\left(\hat{X}_k - \hat{X}_{2,k}\right), \tag{39}$$

where $\beta_{0,k}$ denotes the adaptive factor of one-step state prediction, $\beta_{1,k}$ denotes the adaptive factor of STF_1, and $\beta_{2,k}$ denotes the adaptive factor of STF_2. The adaptive factors are related to the discrepancy between the direct fusion vector and the one-step state prediction, the outputs of local filters. The smaller the deviation is, the larger the adaptive factor. Based on the above assumption, we can consider the adaptive factor as follows

$$\beta_{0,k} = \frac{\frac{1}{||\hat{X}_{k,k-1} - \hat{X}_k^0||_2}}{\frac{1}{||\hat{X}_{k,k-1} - \hat{X}_k^0||_2} + \frac{1}{||\hat{X}_{1,k} - \hat{X}_k^0||_2} + \frac{1}{||\hat{X}_{2,k} - \hat{X}_k^0||_2}}, \tag{40}$$

$$\beta_{1,k} = \frac{\frac{1}{||\hat{X}_{1,k} - \hat{X}_k^0||_2}}{\frac{1}{||\hat{X}_{k,k-1} - \hat{X}_k^0||_2} + \frac{1}{||\hat{X}_{1,k} - \hat{X}_k^0||_2} + \frac{1}{||\hat{X}_{2,k} - \hat{X}_k^0||_2}}, \tag{41}$$

$$\beta_{2,k} = \frac{\frac{1}{||\hat{X}_{k,k-1} - \hat{X}_k^0||_2}}{\frac{1}{||\hat{X}_{k,k-1} - \hat{X}_k^0||_2} + \frac{1}{||\hat{X}_{1,k} - \hat{X}_k^0||_2} + \frac{1}{||\hat{X}_{2,k} - \hat{X}_k^0||_2}}, \tag{42}$$

$$\beta_{0,k} + \beta_{1,k} + \beta_{2,k} = 1. \tag{43}$$

By solving (39), we can get

$$\hat{X}_k = P_{\hat{X}_k}(\beta_{0,k}P^{-1}_{k,k-1}\hat{X}_{k,k-1} + \beta_{1,k}P^{-1}_{1,k}\hat{X}_{1,k} + \beta_{2,k}P^{-1}_{2,k}\hat{X}_{2,k}), \tag{44}$$

then

$$P^{-1}_{\hat{X}_k} = \beta_{0,k}P^{-1}_{k,k-1} + \beta_{1,k}P^{-1}_{1,k} + \beta_{2,k}P^{-1}_{2,k}, \tag{45}$$

where $\hat{X}_k$ is the final fusion results fed back to the INS to give the optimum position and velocity estimation.

IV. EXPERIMENTAL RESULTS AND PERFORMANCE ANALYSIS

A. GENERATION OF TRAJECTORY

Firstly, we generate the real motion information of the vehicle. We set the initial motion parameter of the vehicle as

$$initial = \begin{bmatrix} 0 & 0 & 0 & 5 & 5 & 0 & 36.67 & 116.98 & 0 \end{bmatrix}, \tag{46}$$

where $initial(1:3)$ represents the initial attitude is $0°, 0°, 0°$, $initial(4:6)$ represents the initial velocity is $5m/s$, $5m/s$, $0m/s$, and $initial(7:9)$ represents the initial position is $36.6°N$, $116.98°E$, $0m$.

The vehicle's state information and the trajectory are shown in Table 1 and Fig. 3, respectively.

B. THE PARAMETER SETTING OF THE INTEGRATED NAVIGATION BASED ON RAFSTKF

Through the discussion of section IV, we put the INS error as state variable whose initial value is set as

$$X_{1,0} = X_{2,0} = [O_{1\times 15}]^T, \tag{47}$$

where $X_{1,0}$ represents the initial state value of STF_1, and $X_{2,0}$ represents that of STF_2. Apart from the state variables, we also set the covariance matrix of estimation as

TABLE 1. Vehicle's state information.

duration of movements(s)	state of movements
1–100	moving forward with constant speed
101–200	left turning
201–300	moving forward with constant speed
301–400	right turning
401–500	moving forward with constant speed
501–600	left turning
601–1000	moving forward with constant speed
1001–1100	left turning
1101–1200	moving forward with constant speed

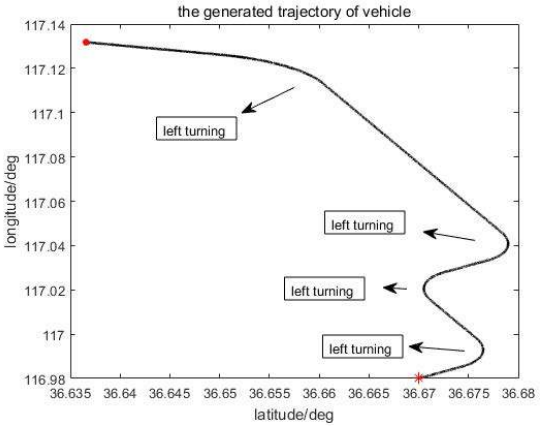

FIGURE 3. The real trajectory of vehicle, where '*' represents the starting point, and '·' represents the ending point.

follows

$$P_{1,0} = P_{2,0} = diag([1.7 \times 10^{-3} \quad 1.7 \times 10^{-3} \quad 1.7 \times 10^{-2} \times 0.1 \quad 0.1 \quad 0.1 \quad 1.6 \times 10^{-6} \quad 1.6 \times 10^{-6} \times 10^{-3} \quad 4.8 \times 10^{-7} \quad 4.8 \times 10^{-7} \quad 4.8 \times 10^{-7} \times 9.8 \times 10^{-3} \quad 9.8 \times 10 \quad 9.8 \times 10^{-3}]^2), \tag{48}$$

where $P_{1,0}$ and $P_{2,0}$ represent estimation covariance matrix of STF_1 and STF_2, respectively.

Q_0 is the initial covariance matrix of the system noise, which can be given by

$$Q_0 = diag([4.8 \times 10^{-8} \quad 4.8 \times 10^{-8} \quad 4.8 \times 10^{-8} \times 9.8 \times 10^{-4} \quad 9.8 \times 10^{-4} \quad 9.8 \times 10^{-4} \times 1.6 \times 10^{-7} \quad 1.6 \times 10^{-7} \quad 1 \quad O_{1\times 6}]^2). \tag{49}$$

R_1 is the covariance matrix of system position measurement noise, and R_2 is the covariance matrix of system velocity measurement noise. Both of them are white Gaussian noise and the initial values are set as

$$R_{1,0} = diag([5 \times 10^{-5} \; 5 \times 10^{-5} \; 10]^2), \tag{50}$$

$$R_{2,0} = diag([0.1 \; 0.1 \; 0.1]^2). \tag{51}$$

C. SIMULATION RESULTS ANALYSIS

Owing to the influence of multipath and the geometry of the satellite positions, GPS is insensitive to attitude. Although DVL has the advantage of getting measured speed in high accuracy, but it cannot give attitude information. Besides, as can be seen from the measurement equations, we mainly focus on the velocity errors of the INS/DVL integrated subsystem and the position errors of the INS/GPS integrated subsystem. We sacrifice attitude information to a certain extent so as to get better position and trajectory. In the meantime, we find that the proposed method has limited improvement in attitude in the simulations. At the same time, considering the fact that the accurate position and tracking are the most important factors cared about in practical applications, the results of the attitude errors are not given in this section.

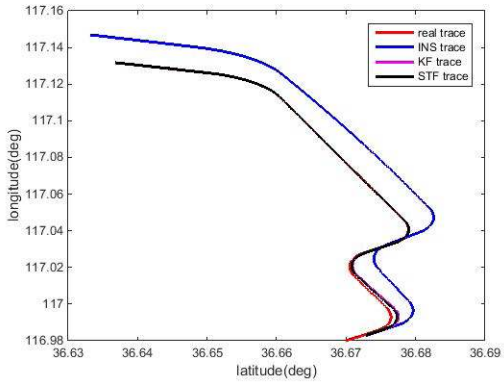

FIGURE 4. Comparison of hybrid federated filter KF based and STF based with accurate model.

1) COMPARISON OF THE HYBRID FEDERATED FILTER KF BASED AND STF BASED

The GPS/INS/DVL integrated navigation simulation results are shown in Fig. 4 and Fig. 5. As depicted in Fig. 4, the STF based method and the KF based method play almost the same role in state estimation when the established system model can faithfully describe the vehicle's motion. However, when we add a bias to the system transition matrix representing that the system model is inaccurate, it is not difficult to find that the hybrid federated filter STF based method outperforms the KF based one in Fig. 5. Although the estimations of STF and KF both have a bias under the case of inaccurate system model, it's easy to find that the error of KF accumulates as time goes by, whereas the error of STF doesn't accumulate, which demonstrates STF still has strong tracking ability even when the system model is inaccurate.

Comparing the trajectory in Fig. 6, we can find that there are some differences between the adaptive fusion results based on the proposed method and INS measurement. At the beginning of the vehicle movement, the proposed method has minor error compared with the real trajectory. The reason is that the influence of the measurement noise has not been

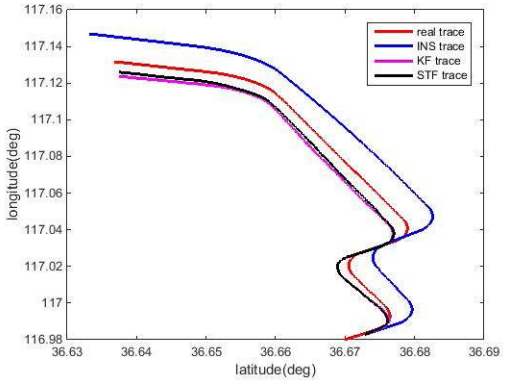

FIGURE 5. Comparison of hybrid federated filter KF based and STF based with inaccurate model.

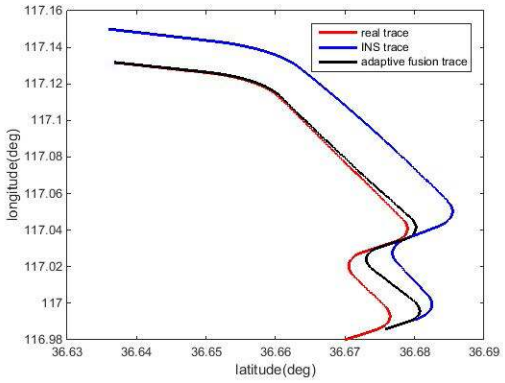

FIGURE 6. Trajectory comparison of INS and adaptive fusion.

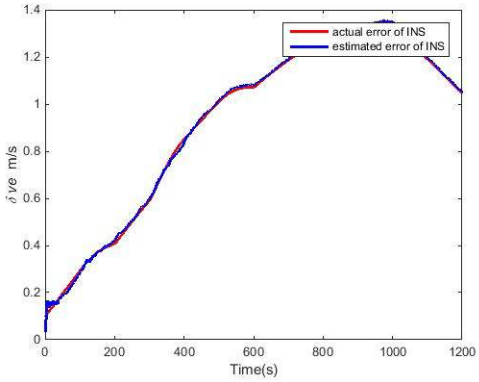

FIGURE 7. Comparison of east velocity error ($T_S = 0.1s$).

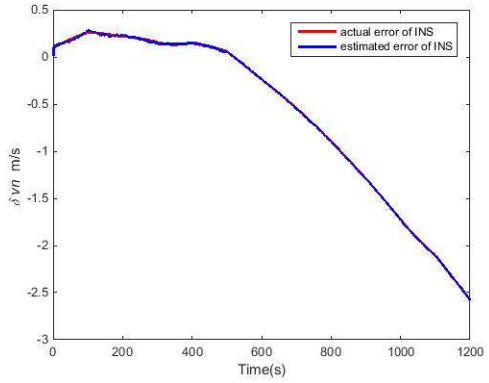

FIGURE 8. Comparison of north velocity error ($T_S = 0.1s$).

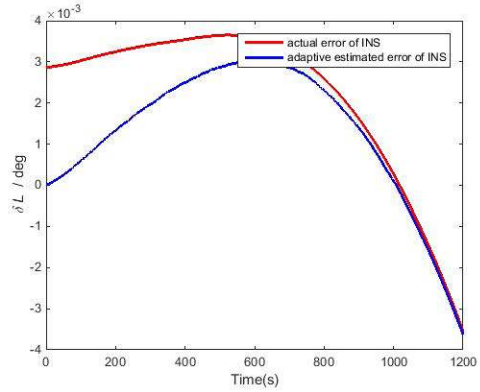

FIGURE 9. Comparison of latitude error ($T_S = 0.1s$).

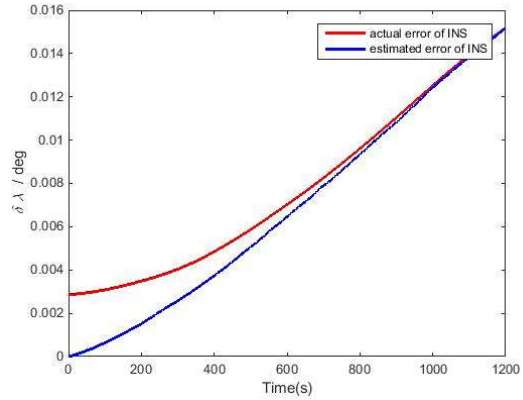

FIGURE 10. Comparison of longitude error ($T_S = 0.1s$).

adjusted. However as time goes by, the adaptive fusion result gets closer to the real trajectory, whereas INS measurement still has large errors compared with the real trajectory. In addition, it's observed that at several turning point, the estimated result of the proposed method is not ideal. The bigger the turning angle is, the worse the result it will get. It can be explained that during the turning periods, the system model established in this paper has much uncertainty and can not describe the vehicle motion accurately.

2) SIMULATION RESULTS OF RAFSTKF

From the results in Fig. 7 to Fig. 10, it can be found that the proposed method can estimate the actual velocity and position error of INS accurately, meanwhile the final navigation results can correct the errors. It is observed in Fig. 7 and Fig. 8 that the estimated velocity errors barely have biases compared with the actual INS errors, whereas the estimated latitude and longitude errors have bigger deviations from the actual one at the beginning as is shown in Fig. 9 and Fig. 10. That's because

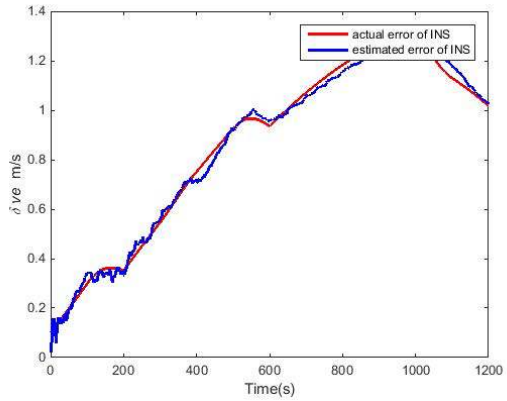

FIGURE 11. Comparison of east velocity error ($T_S = 1s$).

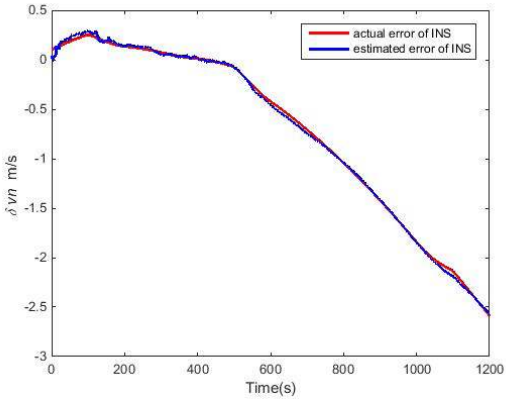

FIGURE 12. comparison of north velocity error ($T_S = 1s$).

the measurement noise plays an important role in simulation results when noise added to velocity is smaller than that added to the position. However, the estimated latitude and longitude error curves get closer to the actual one as time goes by, which demonstrates the proposed adaptive fusion method can improve the positioning accuracy no matter how large the deviation is in the beginning. In addition, although the INS error accumulates over time, the proposed method can correct it accurately.

TABLE 2. MMSE of position.

	MMSE of latitude (deg^2)	MMSE of longitude (deg^2)	MMSE of height (m^2)
direct fusion	1.5124×10^{-6}	1.4734×10^{-6}	0.8399
adaptive fusion	1.5110×10^{-6}	1.4720×10^{-6}	0.7918

To further analyze the proposed adaptive fusion method, we compare the direct fusion method with the adaptive fusion method in Table 2. From the experimental results, we can find that both methods have smaller MMSE than the real one. In addition, the proposed adaptive fusion method still shows superiority over the direct fusion method in latitude, longitude and height.

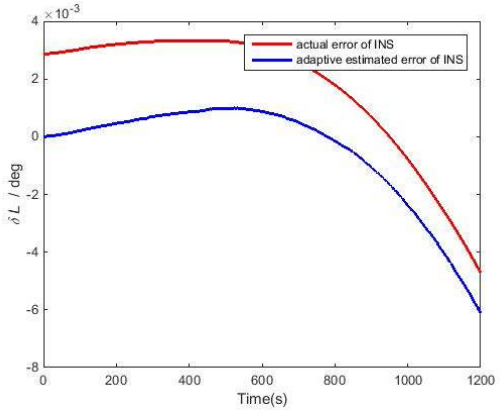

FIGURE 13. Comparison of latitude error ($T_S = 1s$).

TABLE 3. MMSE of position in different sampling intervals.

sampling interval (s)	MMSE of latitude (deg^2)	MMSE of longitude (deg^2)	MMSE of height (m^2)
0.1	1.5110×10^{-6}	1.4720×10^{-6}	0.7918
0.2	2.1416×10^{-6}	2.2554×10^{-6}	1.1028
0.5	3.7136×10^{-6}	3.7235×10^{-6}	2.3117
1	4.9887×10^{-6}	5.1789×10^{-6}	4.5021

3) THE INFLUENCE OF SAMPLING INTERVAL

From the simulation results, it can be found that the sampling interval also has significant impact on the simulation results. Fig. 7 to Fig. 10 are generated with sampling interval $T_s = 0.1s$, while Fig. 11 to Fig. 14 are generated under the condition of sampling interval $T_s = 1s$. Fig. 11 shows that the estimated east velocity error of INS has jitter whereas the estimated north velocity error of INS in Fig. 12 has slight bias. When these inaccurate estimations feedback to INS, it will export imprecise navigation information. However, when the sampling interval is 0.1s, the INS velocity error can be accurately estimated, which will contribute to the final precise navigation. In conclusion, the shorter sampling interval is, the smaller the velocity deviation. We can find the same conclusion in INS position error estimation. As is shown in Fig. 13 and Fig. 14, both the estimated latitude error of INS and estimated longitude error of INS have biases with the actual INS errors, whereas the estimated INS position error converges to the actual one in Fig. 9 and Fig. 10. We compare the MMSE of position in four different sampling durations to rigorously analyze the impact of sampling frequency in Table 3. It is clear that with the increase of the sampling frequency, the MMSE of position becomes smaller and smaller. If the sampling frequency is high, that is to say we can get more information from the measurement, which is advantageous for data update. Moreover, high sampling frequency plays a key role in the establishment of an accurate system model. All of these factors make high sampling frequency output precise navigation information.

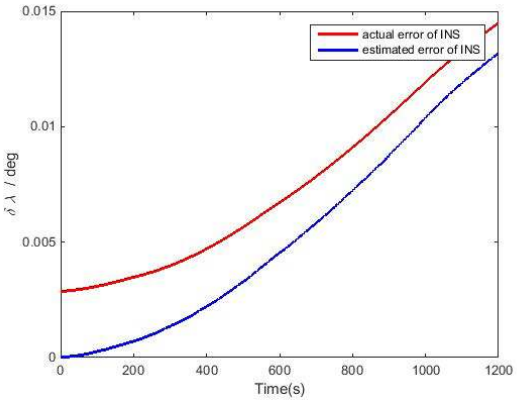

FIGURE 14. Comparison of longitude error ($T_S = 1s$).

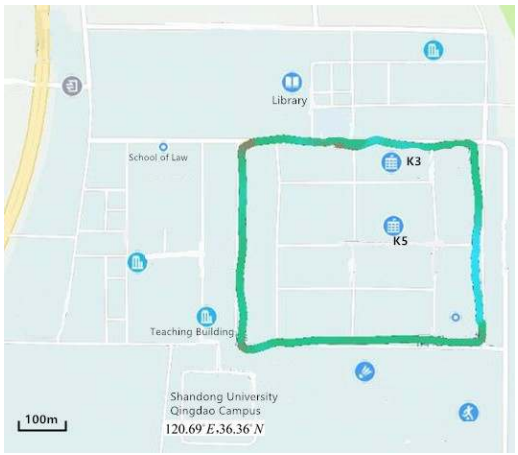

FIGURE 15. The vehicle trajectory in Qingdao campus of Shandong University.

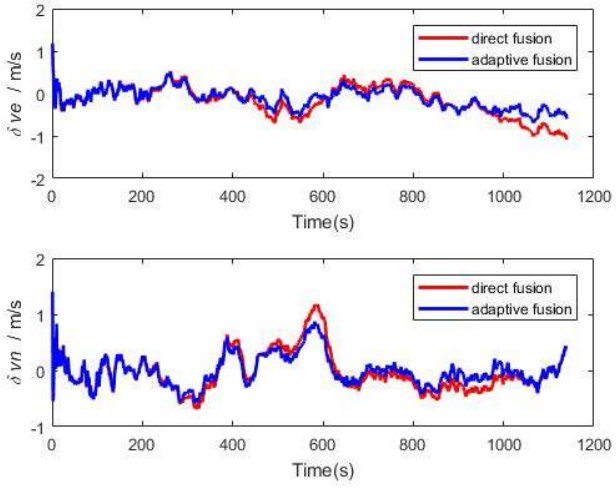

FIGURE 16. Comparisons of east and north velocity errors.

D. PRACTICAL EXPERIMENTAL AND RESULT ANALYSIS

The experiment test was conducted in August 2018 in Qingdao campus of Shandong University, along the street of the campus where dense and tall buildings stand on the side of the road. All the sensors were mounted on the vehicle to collect the raw data of optic gyro based inertial measurement units, including data of gyros and accelerators. The vehicle initial position is the north latitude 36.36°, and the east longitude 120.69°. The trajectory is shown in Fig. 15. Both the traditional KF and the proposed algorithm are performed to compare the performance of the federated filters in this test. The filtering parameters for the two filters are the same as in simulative study.

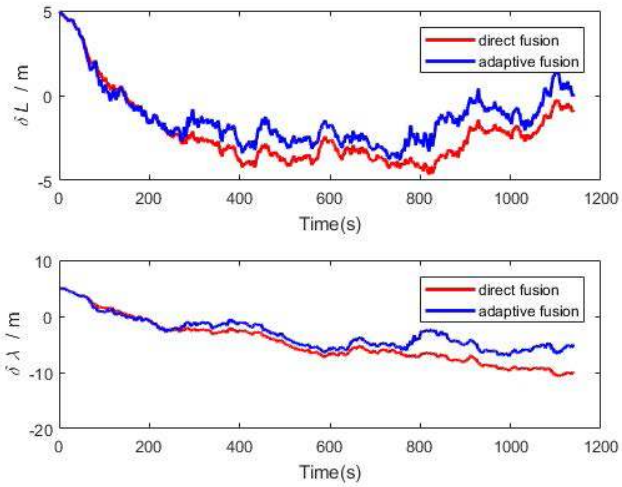

FIGURE 17. Comparisons of latitude and longitude errors.

TABLE 4. MMSE of position in the experiment.

	MMSE of latitude (deg^2)	MMSE of longitude (deg^2)	MMSE of height (m^2)
direct fusion	3.0833×10^{-6}	1.0336×10^{-5}	1.1496
adaptive fusion	1.7397×10^{-6}	6.3976×10^{-6}	1.1308

Since the proposed algorithm has very limited improvement in attitude, we only consider the velocity errors and position errors in this subsection. Fig. 16 and Fig. 17 present the navigation results estimated by the two algorithms in the experiment. As is known, the closer the curve is to zero, the better the effect of the estimation is. It is observed in Fig. 16 that the velocity errors of the two algorithms have slight biases, and the latitude and longitude errors that estimated by the two methods have bigger deviations from each other during the filtering period in Fig. 17. This result is consistent with the conclusion we reached in section IV that the noise added to velocity is smaller than that added to the position. In the meantime, the big jitters in the picture occur around the corners, which is caused by the uncertainty of the system model during the turning periods. Furthermore, the vehicle is easily affected by the hybrid of Gaussian noise and non-Gaussian noise in the natural environment, so there are some deviations in the filtering compared with the results in relatively gentle simulation environment. Table 4 gives the experimental results that can be used to compare the performance of the direct fusion method and the adaptive fusion method. From the experimental results, we can find

that the results are a little higher than that in Table 2, yet we still can get the conclusion that the proposed adaptive fusion method shows superiority over the direct fusion method in latitude, longitude and height.

V. CONCLUSION

In this paper, we propose a novel multi-sensor integrated navigation algorithm based on hybrid GPS/INS/DVL module, which can still provide precise navigation information even when the vehicle moves in less-than-ideal circumstances. The integrated navigation system utilizes the state information of GPS and DVL to correct the INS errors to improve the navigation accuracy. An efficient RAFSTKF algorithm is also presented for data fusion, which has the advantage of robustness with respect to the uncertainty of system model. This paper also introduces the least square principle and adaptively adjusts information sharing factors to obtain the optimal estimation, which can improve the reliability of overall system. The simulation result and practical experiment illustrate that the adaptive fusion method shows superiority over the direct fusion method in terms of the MMSE of position. In addition, the sampling interval also plays an important role in the navigation results. A large number of experimental results show that the shorter the sampling interval is, the better the navigation result will be. Owing to the influence of multipath and the geometry of the satellite positions, GPS is insensitive to attitude, as well as the speed sensitive DVL. The most important accessible performance in this paper is the improvement for positions and trajectory, however, the proposed method has limited improvement in attitude. In the future work, we will focus on improving the performance of the vehicle from three aspects, including attitude, position and velocity.

REFERENCES

[1] M. Z. Win, Y. Shen, and W. Dai, "A theoretical foundation of network localization and navigation," *Proc. IEEE*, vol. 106, no. 7, pp. 1136–1165, Jul. 2018.

[2] A. Soloviev, "Tight coupling of GPS and INS for urban navigation," *IEEE Trans. Aerosp. Electron. Syst*, vol. 46, no. 4, pp. 1731–1746, Oct. 2010.

[3] S. Han, L. Chen, W. Meng, and C. Li, "Improve the security of GNSS receivers through spoofing mitigation," *IEEE Access*, vol. 5, pp. 21057–21069, Oct. 2017.

[4] S. Han, J. Yue, W. Meng, and X. Wu, "A localization based routing protocol for dynamic underwater sensor networks," in *Proc. IEEE Global Commun. Conf.*, Washington, DC, USA, Dec. 2016, pp. 1–6.

[5] H. Xiong, M. Peng, K. Zhu, Y. Yang, Z. Du, and H. Xu, "Efficient bias reduction approach of time-of-flight-based wireless localisation networks in NLOS states," *IET Radar, Sonar Navigat.*, vol. 12, no. 11, pp. 1353–1360, Nov. 2018.

[6] H. Xiong, M. Peng, S. Gong, and Z. Du, "A novel hybrid RSS and TOA positioning algorithm for multi-objective cooperative wireless sensor networks," *IEEE Sensors J.*, vol. 18, no. 22, pp. 9343–9351, Nov. 2018.

[7] T. H. Bryne, J. M. Hansen, R. H. Rogne, N. Sokolova, T. I. Fossen, and T. A. Johansen, "Nonlinear observers for integrated INS/GNSS navigation: Implementation aspects," *IEEE Control Syst. Mag.*, vol. 37, no. 3, pp. 59–86, Jun. 2017.

[8] D. H. Won *et al.*, "Selective integration of GNSS, vision sensor, and INS using weighted DOP under GNSS-challenged environments," *IEEE Trans. Instrum. Meas.*, vol. 63, no. 9, pp. 2288–2298, Sep. 2014.

[9] D. M. Bevly, J. Ryu, and J. C. Gerdes, "Integrating INS sensors with GPS measurements for continuous estimation of vehicle sideslip, roll, and tire cornering stiffness," *IEEE Trans. Intell. Transp. Syst.*, vol. 7, no. 4, pp. 483–493, Dec. 2006.

[10] H. Xiong, S. Wang, S. Gong, M. Peng, J. Shi, and J. Tang, "Improved synchronisation algorithm based on reconstructed correlation function for BOC modulation in satellite navigation and positioning system," *IET Commun.*, vol. 12, no. 6, pp. 743–750, Apr. 2018.

[11] D. J. Jwo and S. H. Wang, "Adaptive fuzzy strong tracking extended Kalman filtering for GPS navigation," *IEEE Sensors J.*, vol. 7, no. 5, pp. 778–789, May 2007.

[12] S. Wang, Z. Deng, and Y. Gang, "An accurate GPS-IMU/DR data fusion method for driverless car based on a set of predictive models and grid constraints," *Sensors*, vol. 16, no. 3, pp. 280–292, Feb. 2016.

[13] J. Kichun, C. Keounyup, and S. Myoungho, "Interacting multiple model filter-based sensor fusion of GPS with in-vehicle sensors for real-time vehicle positioning," *IEEE Trans. Intell. Transp. Syst.*, vol. 13, no. 1, pp. 329–343, Mar. 2012.

[14] A. Tai, I. Klein, and R. Katz, "Inertial navigation system/Doppler velocity log (INS/DVL) fusion with partial DVL measurements," *Sensors*, vol. 17, no. 2, pp. 415–435, Feb. 2017.

[15] Q. Wang, X. Cui, Y. Li, and Y. Ye, "Performance enhancement of a USV INS/CNS/DVL integration navigation system based on an adaptive information sharing factor federated filter," *Sensors*, vol. 17, no. 2, pp. 239–265, Feb. 2017.

[16] M. Romanovas, R. Ziebold, and L. Lanca, "A method for IMU/GNSS/Doppler velocity log integration in marine applications," in *Proc. Int. Assoc. Inst. Navigat. World Congr.*, Prague, Czech Republic, Oct. 2015, pp. 1–8.

[17] H. Xiong, W. Zhang, Z. Du, B. He, and D. Yuan, "Front-end narrowband interference mitigation for DS-UWB receiver," *IEEE Trans. Wireless Commun.*, vol. 12, no. 9, pp. 4328–4337, Sep. 2013.

[18] H. Xiong, "An efficient narrowband interference suppression approach in ultra-wideband receiver," *IEEE Sensors J.*, vol. 17, no. 9, pp. 2741–2748, Sep. 2013.

[19] H. Xiong and J. Cheng, "Investigation of short-range high precision 3D localization via UWB radio," in *Proc. IEEE Global Commun. Conf.*, Austin, TX, USA, Dec. 2014, pp. 4090–4095.

[20] S. Gezici *et al.*, "Localization via ultra-wideband radios: A look at positioning aspects for future sensor networks," *IEEE Signal Process. Mag.*, vol. 22, no. 4, pp. 70–84, Jul. 2005.

[21] J. Xu, M. Ma, and C. L. Law, "Position estimation using ultra-wideband time difference of arrival measurements," *IET Sci., Meas. Technol.*, vol. 2, no. 1, pp. 53–58, Jan. 2008.

[22] L. Zhao, H. Qiu, and Y. Feng, "Analysis of a robust Kalman filter in loosely coupled GPS/INS navigation system," *Measurement*, vol. 80, pp. 138–147, Feb. 2016.

[23] J. N. Gross, Y. Gu, and M. B. Rhudy, "Robust UAV relative navigation with DGPS, INS, and peer-to-peer radio ranging," *IEEE Trans. Autom. Sci. Eng.*, vol. 12, no. 3, pp. 935–944, Jul. 2015.

[24] S. P. Karatsinides, "Enhancing filter robustness in cascaded GPS-INS integrations," *IEEE Trans. Aerosp. Electron. Syst.*, vol. 30, no. 4, pp. 1001–1008, Oct. 1994.

[25] K. Li, J. Zhao, X. Wang, and L. Wang, "Federated ultra-tightly coupled GPS/INS integrated navigation system based on vector tracking for severe jamming environment," *IET Radar, Sonar Navigat.*, vol. 10, no. 6, pp. 1030–1037, 2016.

[26] A. M. Rad, J. H. Nobari, and A. A. Nikkhah, "Optimal attitude and position determination by integration of INS, star tracker, and horizon sensor," *IEEE Aerosp. Electron. Syst. Mag.*, vol. 29, no. 4, pp. 20–33, Apr. 2014.

[27] X. Wang, N. Cui, and J. Guo, "INS/VisNav/GPS relative navigation system for UAV," *Aerosp. Sci. Technol.*, vol. 28, no. 1, pp. 242–248, Jul. 2013.

[28] B. Yang, K. V. Katsaros, W. K. Chai, and G. Pavlou, "Cost-efficient low latency communication infrastructure for synchrophasor applications in smart grids," *IEEE Syst. J.*, vol. 12, no. 1, pp. 948–958, Mar. 2018.

[29] B. Yang, W. K. Chai, Z. Xu, K. V. Katsaros, and G. Pavlou, "Cost-efficient NFV-enabled mobile edge-cloud for low latency mobile applications," *IEEE Trans. Netw. Service Manage.*, vol. 15, no. 1, pp. 475–488, Mar. 2018.

[30] J. Simanek, M. Reinstein, and V. Kubelka, "Evaluation of the EKF-based estimation architectures for data fusion in mobile robots," *IEEE/ACM Trans. Mechatronics*, vol. 20, no. 2, pp. 985–990, Apr. 2015.

[31] H. Xiong, J. Tang, H. Xu, W. Zhang, and Z. Du, "A robust single GPS navigation and positioning algorithm based on strong tracking filtering," *IEEE Sensors J.*, vol. 18, no. 1, pp. 290–298, Jan. 2018.
[32] K. H. Kim, J. G. Lee, and C. G. Park, "Adaptive two-stage extended Kalman filter for a fault-tolerant INS-GPS loosely coupled system," *IEEE Trans. Aerosp. Electron. Syst.*, vol. 45, no. 1, pp. 125–137, Jan. 2009.
[33] B. Cui, X. Chen, and X. Tang, "Improved cubature Kalman filter for GNSS/INS based on transformation of posterior sigma-points error," *IEEE Trans. Signal Process.*, vol. 65, no. 11, pp. 2975–2987, Jun. 2017.
[34] J. Huang and H. S. Tan, "A low-order DGPS-based vehicle positioning system under urban environment," *IEEE/ASME Trans. Mechatronics*, vol. 11, no. 5, pp. 567–575, Oct. 2006.
[35] D. H. Zhou and P. M. Frank, "Strong tracking filtering of nonlinear time-varying stochastic systems with coloured noise: Application to parameter estimation and empirical robustness analysis," *Int. J. Control*, vol. 65, no. 2, pp. 295–307, Oct. 1996.
[36] C. L. Lin, Y. M. Chang, C. C. Hung, C. D. Tu, and C. Y. Chuang, "Position estimation and smooth tracking with a fuzzy-logic-based adaptive strong tracking Kalman filter for capacitive touch panels," *IEEE Trans. Ind. Electron.*, vol. 62, no. 8, pp. 5097–5108, Aug. 2015.
[37] J. Li, R. Zhao, J. Chen, C. Zhao, and Y. Zhu, "Target tracking algorithm based on adaptive strong tracking particle filter," *IET Sci., Meas. Technol.*, vol. 10, no. 7, pp. 704–710, Sep. 2016.
[38] N. A. Carlson, "Federated square root filter for decentralized parallel processors," *IEEE Trans. Aerosp. Electron. Syst.*, vol. 26, no. 3, pp. 517–525, May 1990.
[39] D. Zhou, Y. Xi, and Z. Zhang, "A suboptimal multiple fading extended Kalman filter," *Acta Astronaut. Sinica*, vol. 17, no. 6, pp. 689–695, Nov. 1991.
[40] M. Fu, Z. Deng, and L. Yan, "Practical Kalman filtering technology," in *Kalman Filter Theory and Its Application in Navigation System*, vol. 4, 2nd ed. Beijing, China: Science Press, 2003, pp. 98–100.
[41] T. Xu, Q. Ge, X. Feng, and C. Wen, "Strong tracking filter with bandwidth constraint for sensor networks," in *Proc. IEEE Int. Conf. Control Autom.*, Xiamen, China, Jun. 2010, pp. 596–601.
[42] Z. Yin, G. Li, X. Sun, J. Liu, and Y. Zhong, "A speed estimation method for induction motors based on strong tracking extended Kalman filter," in *Proc. IEEE Int. Power Electron. Motion Control Conf.*, Hefei, China, May 2016, pp. 798–802.

HAILIANG XIONG (M'11) received the B.Sc. and Ph.D. degrees in communication and information systems from Xidian University, Xi'an, China, in 2005 and 2011, respectively. From 2009 to 2011, he was a Visiting Scholar with the University of Sheffield, U.K., and the University of Bedfordshire, U.K. From 2014 to 2015, he held a postdoctoral position with The University of British Columbia, Canada. He is currently an Associate Professor with the School of Information Science and Engineering, Shandong University, Qingdao, China. His research interests include navigation and positioning, satellite communications, cognitive radio networks, interference suppression, electronic warfare, and artificial intelligence algorithms.

ZHENZHEN MAI (S'19) received the B.Sc. degree from the College of Communication and Information Engineering, Chongqing University of Posts and Telecommunication, Chongqing, China, in 2013. She is currently pursuing the M.S. degree with the School of Information Science and Engineering, Shandong University, Qingdao, China. Her research interests include satellite navigation and positioning, integrated navigation, information fusion, artificial intelligence, adaptive filter, intelligent transportation, and deep learning.

JUAN TANG received the B.Sc. degree from the College of Information and Electrical Engineering, China Agricultural University, Beijing, China, in 2015, and the M.S. degree from the School of Information Science and Engineering, Shandong University, Jinan, China, in 2018. She is currently a Government Staff in Nantong, Jiangsu. Her research interests include navigation and positioning, indoor positioning, hybrid navigation, integrated navigation, and information fusion.

FEN HE received the bachelor's and master's degrees from the School of Political Economics, Shaanxi Normal University, Xi'an, China, in 2009 and 2012, respectively. She has been a Financial Analyst and an Engineer with Aerospace Jiutong Internet of Vehicles Co., Ltd., successively.

She is currently a Staff with the School of Information Science and Engineering, Qingdao Campus, Shandong University, Qingdao, China. Her research interests include information management, supply-chain management, mathematical statistics, satellite navigation and positioning, and intelligent transportation.